EUR 5157 e

COMMISSION OF THE EUROPEAN COMMUNITIES

MONTECARLO CALCULATIONS FOR THE MODERATOR OF THE PULSED NEUTRON TARGET OF THE GEEL LINAC

by

A. BIGNAMI, C. COCEVA and R. SIMONINI (CNEN)

1974

Report prepared by CNEN
Comitato Nazionale per l' Energia Nucleare (CNEN) – Bologna (Italy)

Euratom Contract No. 001 – 69 – PIPGI/01 – 72 COLL – B/BCNM

This report is on sale at the addresses listed on cover page 4

at the price of B.Fr. 50.

Commission of the European Communities
D.G. XIII - C.I.D.
29, rue Aldringen
L u x e m b o u r g
September 1974

EUR 5157 e

COMMISSION OF THE EUROPEAN COMMUNITIES

EUR 5157 e

MONTECARLO CALCULATIONS FOR THE MODERATOR OF THE PULSED NEUTRON TARGET OF THE GEEL LINAC
by A. BIGNAMI, C. COCEVA, R. SIMONINI

Commission of the European Communities
Report prepared by CNEN
Comitato Nazionale per l'Energia Nucleare (CNEN), — Bologna (Italy)
Euratom Contract No. 001-69-PIPGI/01-72 COLL-B/BCNM
Luxembourg, September 1974 — 38 Pages — 18 Figures — B.Fr. 50.—

The results are reported of Montecarlo calculations which were performed to compare the characteristics of two different dispositions of the moderator near the pulsed neutron target of the Geel linear accelerator for neutron time-of-flight experiments.

The resolution function is obtained for the disposition eventually chosen. The effect of different flight-path directions on the resolution is evaluated.

[ODERATOR OF
GEEL LINAC

NEN)

EUR 5157 e

MONTECARLO CALCULATIONS FOR THE MODERATOR OF THE PULSED NEUTRON TARGET OF THE GEEL LINAC
by A. BIGNAMI, C. COCEVA, R. SIMONINI

Commission of the European Communities
Report prepared by CNEN
Comitato Nazionale per l'Energia Nucleare (CNEN), — Bologna (Italy)
Euratom Contract No. 001-69-PIPGI/01-72 COLL-B/BCNM
Luxembourg, September 1974 — 38 Pages — 18 Figures — B.Fr. 50.—

The results are reported of Montecarlo calculations which were performed to compare the characteristics of two different dispositions of the moderator near the pulsed neutron target of the Geel linear accelerator for neutron time-of-flight experiments.

The resolution function is obtained for the disposition eventually chosen. The effect of different flight-path directions on the resolution is evaluated.

Report prepared by CNEN
Comitato Nazionale per l' Energia Nucleare (CNEN) – Bologna (Italy)

Euratom Contract No. 001 – 69 – PIPGI/01 – 72 COLL – B/BCNM

It is oriented to analize the escaped particles.
The geometry treatment is made by the O5R code's routines [1] , which allow configurations which can be described by combinations of quadric surfaces.
The nuclear reactions taken into account are scattering, both elastic and inelastic, fission and radiative capture, treated by the RAM code's routines [2] .
Elastic scattering may be both isotropic and anisotropic in the C.M. system.
Inelastic scattering may be treated according to three different models: excitation of known discrete energy levels, evaporation model, transition matrix (i.e. matrix of scattering probabilities from one energy group to another). The energy range of interest may be covered by the first or the second model and also by both for the same isotope; the third model does not admit any alternative.
Fission is treated by multiplying the statistical weight of the particle by the probable number of fission-neutrons. The energy of the outcoming particle is assumed to be independent of the energy before collision, and is sampled from the Rosen distribution [2]
Radiative capture is taken into account by reducing the statistical weight according to the capture probability at each collision.
The code is provided with a library of data taken from UKNDL, febr. 1968.
In order to sample the source-neutrons, two routines must be written, one for the space and another for

the energy distribution, providing the starting parameters of each neutron for the given problem.
The transport simulation makes use of the "forced collision" device: at birth each particle is given an unitary statistical weight; a fraction of weight equal to the escape probability is removed from the system, while the remaining fraction is forced to undergo a collision within the system. This device is applied after each collision until the statistical weight falls under a given cut-off value: in this case the history is terminated. A history may also end when the energy falls under a given cut-off value.
In order to put in evidence differential effects in different systems, the chains of random numbers used in the cases to be compared are correlated: corresponding histories (i.e. having the same ordinal number) start with the same pseudorandom number [3] .
If at birth the escape probability is one(i.e. the trajectory of the source-neutron lies entirely in vacuum), the neutron is not followed and does not contribute to the estimation of the required quantities. Histories for which the escape probability at birth is less than one are called "useful histories". All calculated probabilities are normalized to the number of useful histories.
The program output gives the average number of collisions per useful history, the capture probability in the different media, the escape probability and the

probability that a history be terminated by energy or weight cut-off. The code provides also a group spectrum of the escaped neutrons independently of their direction and position, and the probability that the direction be in a given cone around the normal to the moderator face. Besides, for neutrons escaped in this cone and for each of the required energy groups, the following quantities are given:

1) number of escaped neutrons;

2) average and variance of the product of the escape velocity v_u times the time t during which the neutron stays in the system; this product $v_u t = d$ is called "moderation distance" †) .

3) the distribution of the escape coordinate x, discretized in intervals of equal length (see the example of fig. 3A, where the moderator surface is divided in ten strips). This distribution is necessary to obtain the resolution function for slanting flight-paths;

4) the distribution of the moderation distance d discretized in intervals of equal length, also plotted if required.

---

†) The effective fligh distance L, defined as the product of the time of flight and the neutron velocity, is obtained by adding d to the distance travelled by the neutron from the surface of the moderator to the detector. This implies that the time of flight starts at the neutron birth in the Uranium target.

3 - Comparison of two different configuations.

The two moderator configuartions which have been compared are similar to those described in ref. [4] and in ref. [5] . The first configuration is illustrated in fig. 1: the solid angle under which the fast-neutron source sees the moderator is maximized, and two different moderator slabs are used for the flight paths at the right and at the left of the electron beam. The two slabs must be decoupled by means of neutron-absorbing material in order to suppress the moderated neutrons flying back from one slab to the other.

The second configuration is illustrated in fig. 2: the same slab is used for flight paths on both sides. A shadow-shield placed at the same height as the Uranium target scatters out all neutrons coming directly from the target in the direction(horizontal) of the flight-paths, so that the samples can be reached only by neutrons issued from the moderator. The solid angle under which the fast-neutron source sees the moderator is smaller in this case, but one gains two important advantages over the double slab disposition

1) the troubles due to the double source of moderated neutrons are completely avoided.

2) The γ-flash and the fast-neutron dose on the detectors are strongly reduced.

In the calculations, the extended source of fast neutrons was approximated with three point sources with equal strengths, placed in a row on the axis of the Uranium target, as indicated in fig. 4. The fast-neutron source was assumed to be isotropic with a mixed evaporation and fission spectrum, as specified in [6.]
In these first calculations, the effect of Carbon atoms in the polyethylene moderator was neglected: only Hydrogen was taken into account. In the configuration of fig. 1 each Boron layer had a thickness of 1 cm, with 1 g/cm^2 of ^{10}B.
Montecarlo calculations were carried out for the double slab case with dimensions indicated in fig. 1 and for three different thicknesses of the single slab configuration: these thicknesses were 2, 3 and 4 cm, the other dimension are indicated in fig. 2 .
For the double slab case, the solid angle under which the fast-neutron source sees the moderator is Ω =72%; for the three thicknesses of the single slab configuration, the solid angles are Ω = 30%, 41%, and 49%, respectively.
Neutrons emitted from the moderator are classified in six equal lethargy intervals from 3 eV to 3 MeV. Tab. 1 and fig. 5 give the moderator efficiency $\epsilon(n)$ i.e. the number of neutrons in the n-th interval leaving the moderator in a solid angle of one steradian around the normal to the moderator face; this number is normalized to one source-neutron.
Besides the obvious increase of efficiency with thickness for the single slab case, two features are

immediately apparent: first, the double slab configuration yields a larger number of neutrons in the useful energy range; second, fast neutrons above 0.3 MeV are strongly suppressed in the single slab configuration. This is true even if actually this effect is not as high as shown, because in these calculations the effect of Carbon atoms in polyethylene was neglected.

Table 2 reports the variance of the distribution of the moderation distance. For the single slab configuration var d is obviously increasing with thickness. In the case of the double slab configuration, var d is much larger, with the exception of the first two energy intervals. This means that, in spite of the two enriched Boron layers, neutron reflections between the two slabs cause a long tail in the distribution of the moderation distance already at rather low energies.

Table 3 gives the values of the figure of merit, M(n), i.e. the ratio between the moderator efficiency and the variance of the moderation distance. The results show that the three thicknesses of the single slab configuration are practically equivalent, since var d increases with thickness approximately as the efficiency. The double slab configuration shows to be less convenient in the most interesting energy range, i.e. from 300 eV to 300 keV. In view of the above results and of various other considerations the single slab configuration with a thickness of 4 cm was adopted for the Geel linac.

4 - Characteristics of the Geel moderator

Fig. 6 shows schematically the moderator-target assembly; a cutaway view is given in fig. 4.
A Montecarlo calculation was carried out with the main purpose of deducing the resolution function for this set-up. To this end, an accurate description of the distribution of the moderation distance d in each energy interval must be obtained: satisfactory statistical accurancy was reached with 130,000 histories corresponding to 64,300 useful histories. In this calculation it was assumed that the polyethylene moderator is a homogeneous mixture of 0.80 g cm^{-3} of Carbon and 0.13 g cm^{-3} of Hydrogen.
The main results are summarized in tab. 4, which gives the moderator efficiency $\epsilon(n)$ †), the average moderation distance $\langle d \rangle$, the variance of the moderation distance var d, and the width $\Delta d_{1/2} = 2.355\,(\mathrm{var}\ d)^{1/2}$ of the distribution of the moderation distance *).
The energy spectrum N(E) of the neutrons issuing from the moderator in a cone of one steradian is shown in fig. 7. Between 100 eV and 10 keV the spectrum is well represented by the following expression

$$N(E) = 6.8\ 10^{-4}\ E^{-0.834}\ eV^{-1}\ sr^{-1} \quad [\,E \text{ in eV}\,] \qquad (1)$$

---

†) The difference between these values of ϵ and those given in the last column of tab. 1 is mainly due to the fact that this calculation does take into account the effect of Carbon atoms in the moderator.

*) The factor $2.355 = (8 \ln 2)^{1/2}$ is the ratio between FWHM and standard deviation for a gaussian distribution.

The behaviour of the average moderation distance $<d>$ as a function of neutron energy is shown in fig. 8 . The variation of $<d>$ means that the effective mean flight-distance $\bar{L} = L_0 + <d>$ is an energy-dependent quantity; $\bar{L}$ is increasing with increasing neutron energy. For calculation purposes, the following expression may be adopted

$$<d> = 0.017 \qquad \text{for } E < 120 \text{ eV}$$

$$<d> = 0.017 + 1.77 \; 10^{-3} (\log_{10} E - 2.08)^2 \quad \text{for } E > 120 \text{ eV} \qquad 2)$$

where $<d>$ is espressed in m and E in eV.
The histograms of figs. 9 - 14 represent the calculated distributions of the deviation of the moderation distance from its mean value : $d' = d - <d>$. For flight-paths perpendicular to the moderator face, the histograms describe that part of the resolution function which is due to the moderation of the source-neutrons.
In order to put the distribution of d in a form suitable for use in shape anlysis of t.o.f. spectra, the histograms were fitted empirically with curves being basically χ^2 -functions with an appropriate number ν of degrees of freedom. We use here the definition of χ^2 -function in an extended sense, including non-integer values of ν. Let us consider a

variable z having a χ^2-distribution:

$$f(z) = \frac{z^{\nu/2 - 1}}{2^{\nu/2}\,\Gamma(\nu/2)} \; e^{-z/2} \qquad (3)$$

and determine a simple relation between z and d, depending on a small number of free parameters and accounting for the deviation of the distribution of d from a χ^2-function. The fitting procedure will determine the best values of the free parameters, including ν. Actually, for each of the first three energy intervals, i.e. from 3 eV to 3 keV, a good fit is obtained with (3), performing a linear change of scale:

$$d = a_1 z \qquad (4)$$

As we have the Montecarlo evaluation of two momenta of the distribution of d, i.e. the average and the variance, the two free parameters a_1 and ν can be determined straightforwardly by equating to these estimates the corresponding momenta of the curve. One gets:

$$a_1 = \frac{\langle d \rangle}{\nu} \qquad \text{and} \quad \nu = \frac{2 \langle d \rangle^2}{\text{var } d} \qquad (5)$$

where $\langle d \rangle$ and var d are the Montecarlo estimates. As one can see from figs. 9-11, such fitting criterion gives also a very good shape fit. This is not surprising since a χ^2-function with $\nu = 6$ degrees of freedom is the theoretical shape deduced by Groenewold and Greondijk [7] for an infinite non-absorbing hydrogenous moderator; in this case one obtains $\langle d \rangle = 3\lambda_H$, where λ_H is the neutron mean free path in the moderator. In our case, at low neutron energy, we obtain $\nu \simeq 7$ and $\langle d \rangle = 1.7$ cm $\cong 3\lambda_{CH_2}$, where λ_{CH_2} is the mean free path in polyethylene.

For the other three energy intervals, i.e. from 3 keV to 3 MeV, a cubic relation between z and d was introduced to account for the increasing skewness of the histograms:

$$d = a_o + a_1 z + a_2 z^2 + a_3 z^3 \quad . \qquad (6)$$

The coefficients a_o, a_1, a_2, a_3 and the ν value were deduced in these cases by means of the least-square fitting procedure. Consequently, the variance and the average values of d are not exactly coincident with those of the corresponding histograms. The fitsare given in figs. 12 - 14.

The coefficients of the transformation (6) and the number of degrees of freedom ν obtained for each energy interval are given in tab. 5 .

In the case of flight-paths not perpendicular to the moderator slab, an additional contribution to the flight-distance uncertainty must be taken into account. In fact for such flight-paths the flight-distance travelled by a given neutron depends on the x value of the exit point from the moderator (see fig. 3). For this reason, in the calculations, the moderator slab was divided in ten vertical slices 1.5 cm wide, and for each of them the Montecarlo program supplied the values ϵ_x, var d_x and $\langle d_x \rangle$.

The x-dependence of the neutron intensity was found to be the same, within the errors, for all energy intervals: the distribution p(x) of the escape x coordinate is shown in fig. 15. It was also found that the variation of $\langle d_x \rangle$ with x is approximately linear : $\langle d_x \rangle$ is minimum at the centre of the moderator, i.e. at x = 0 and it is maximum at the edges, i.e. at x = ± 7.5 cm. The variation of $\langle d_x \rangle$ across the moderator face increases with neutron energy. Neutrons leaving the moderator at x, with direction defined by θ (see fig.3), travel an effective mean flight-distance $\bar{L}_x(\theta) = L_o + x \sin\theta + \langle d_x \rangle$.

The quantity $\Delta l(\theta,x) = \bar{L}_x(\theta) - \bar{L}$ describes the variation along x of the local value of the effective mean flight-distance. Figs. 16 and 17 show for two different angles θ of the flight-paths and for each energy interval the distribution $p(\Delta l)$ of $\Delta l(\theta,x) =$ $= x \sin\theta + \langle d_x \rangle - \langle d \rangle$.

The histograms of figs. 16 and 17 describe that part of the resolution function which is due to the deviation of the flight-path direction from the normal to the moderator face. For calculation purposes the same data are reported in tabs. 6 and 7.

Because of the systematic behaviour of $<d_x>$ with x, it would be uncorrect to fold this part of the resolution function with p(d') (figs. 9 - 14) in order to obtain the distribution of the effective flight-distance. An approximate way of dealing with this problem is to shrink the curves of figs. 9 -14 along d' by a factor

$$C = \frac{< (\text{var } d_x)^{1/2} >}{(\text{var } d\ )^{1/2}} \qquad (7)$$

where $<(\text{var } d_x)^{1/2}>$ is the average over x of $(\text{var } d_x)^{1/2}$ weighted on ϵ_x. It is found that the above correction factor can be neglected for neutron energies below 0.3 MeV; it results C = 0.99 for all energies up to 0.3 MeV, and C = 0.92 for the interval 0.3 - 3 MeV. For slanting flight-paths, the corrected parameters of the functions to be folded with the distribution of figs. 16 and 17 (Tabs. 6 and 7) are given in tab. 5 .

The time width $\Delta t_{1/2}$ of the combined distribution of d and Δ l is plotted in fig. 18 for three values of the flight-path angle $\theta = 0^o$, 9^o and 18^o: it was assumed

$$\Delta t_{1/2} = 722.96\ E^{-1/2}\ 2.355\ (\text{var } d)^{1/2} \qquad \text{for } \theta = 0^o$$

$$\Delta t_{1/2} = 722.96\ E^{-1/2}\ 2.355\ (<\text{var } d_x> + \text{var } \Delta l(\theta))^{1/2} \text{ for } \theta \neq 0 \qquad (8)$$

[$\Delta t_{1/2}$ in nsec: E in eV; d, d_x, Δ l in cm] .

Acknowledgments

Useful discussions with P.Giacobbe and M.Stefanon are gratefully acknowledged.

Thanks are also due to G.C.Panini for the preparation of the cross-section library.

List of symbols

a_0, a_1, a_2, a_3	: Coefficients of the transformation(6). $d = a_0 + a_1 z + a_2 z^2 + a_3 z^3$
d	: moderation distance . $d = v_u t$.
$<d>$	: mean value of d.
d'	: deviation of d from $<d>$. $d' = d - <d>$
$d_{x'}$	: moderation distance for a neutron escaping at $x = x'$.
$<d_x>$	: mean value of d_x .
$\Delta d_{1/2}$	: width of the distribution of d. $\Delta d_{1/2} = (8 \ln 2)^{1/2} (\mathrm{var}\ d)^{1/2} = 2.355 (\mathrm{var}\ d)^{1/2}$.
$\Delta t_{1/2}$	: width of the time-of-flight distribution. $\Delta t_{1/2} = (8 \ln 2)^{1/2} (\mathrm{var}\ t)^{1/2} = 2.355 (\mathrm{var}\ t)^{1/2}$.
$\Delta l\ (\theta, x)$	: deviation of $\bar{L}_x(\theta)$ from $\bar{L}$. $\Delta l(\theta,x) = \bar{L}_x(\theta) - \bar{L}$
$\epsilon(n)$	: Moderator efficiency in the n-th energy interval. $\epsilon(n) = \int_{3\times10^{n-1}}^{3\times10^{n}} N(E)\ dE$
θ	: angle between the direction of a flight-path and the normal to the moderator face. The convention about the sign of θ is indicated in fig. 3
L_o	: geometric flight-distance, i.e. distance between the neutron detector and the centre of the outer face of the moderator.

L : effective flight-distance. $L = L_o + d$

$\bar{L}$: mean value of L . $\bar{L} = L_o + \langle d \rangle$

$L_{x'}(\theta)$: effective flight-distance for neutrons escaping at $x = x'$. $L_x(\theta) = L_o + x \sin\theta + d_x$

$\bar{L}_x(\theta)$: mean value of L_x . $\bar{L}_x = L_o + x \sin\theta + \langle d_x \rangle$

$M(n)$: figure of merit for the n-th energy interval. $M(n) = (\varepsilon/\text{var } d)_n$

$N(E)$: energy spectrum, i.e. number of neutrons per unit energy interval escaping within one steradian around the normal to the moderator face. N(E) is normalized to one source-neutron.

N_{coll} : average number of collisions per source--neutron within the solid angle Ω .

ν : number of degrees of freedom of the χ^2 function (3).

$p(d')$, $p(\Delta l)$, $p(x)$: diffential probability distributions; e.g. $p(x')\,dx$ is the probability that the escape x-coordinate be in the interval dx around the value x'.

t : delay time between production and exit of a neutron from the target-moderator system.

v_u : velocity of a neutron escaping from the system.

Ω : solid angle under which the fast-neutron source sees the moderator.

References.

1 - D.C. Irving et al. "05R A general-purpose Monte Carlo neutron transport code "ORNL-3622(1965).

2 - E.Cupini, A.De Matteis. "RAM - An IBM-7094 Monte Carlo code for criticality calculations" RT/FIMA (65)5.

3 - G.Cenacchi, A.De Matteis. Num.Math. 16 (1970) 11.

4 - A.Michaudon - Journ.of Nucl.Energy, Parts A-B, 17 (1963)165.

5 - R.L.Macklin - Nucl.Instr. and Meth., 91 (1971)79.

6 - J.D.King - "Production of neutrons for time-of--flight work with the Saskatchewan linear accelerator" Internal report n. 6 (Revised)(1963).

7 - H.J.Groenewold and H.Groendijk, Physica, 13 (1947)141.

Table 1 - Moderation efficiency: ϵ (n) (sr^{-1})

Interval	Energy	Double	Single slab		
n		slab	2 cm	3 cm	4 cm
1	3 - 30 eV	2.43×10^{-3}	0.80×10^{-3}	1.50×10^{-3}	2.04×10^{-3}
2	30 - 300 eV	3.38x "	1.47x "	2.32x "	2.93x "
3	0.3 - 3 keV	5.49x "	2.63x "	3.77x "	4.41x "
4	3 - 30 keV	8.86x "	4.76x "	6.40x "	7.29x "
5	30 - 300 keV	22.27x "	9.82x "	13.45x "	15.77x "
6	0.3 - 3 MeV	96.50x "	3.15x "	6.11x "	9.50x "

Double slab Ω = 72% ; N_{coll} = 2.37

Single slab, 2 cm Ω = 30% ; N_{coll} = 1.40

Single slab, 3 cm Ω = 41% ; N_{coll} = 1.76

Single slab, 4 cm Ω = 49% ; N_{coll} = 2.09

Table 2 - Variance of the moderation distance : var d (cm^2).

Interval n	Energy	Double slab	Single slab		
			2 cm	3 cm	4 cm
1	3 - 30 eV	0.57	0.34	0.53	0.74
2	30 - 300 eV	0.67	0.38	0.60	0.80
3	0.3 - 3 keV	1.40	0.44	0.66	0.85
4	3 - 30 keV	3.54	0.50	0.67	0.81
5	30 - 300 keV	7.72	0.77	0.98	1.14
6	0.3 - 3 MeV	5.29	1.09	1.14	1.05

Table 3 - Figure of merit : M(n) (sr^{-1} cm^{-2}).

Interval n	Energy	Double slab	Single slab 2 cm	Single slab 3 cm	Single slab 4 cm
1	3 - 30 eV	4.0x10^{-3}	2.3x10^{-3}	2.8x 10^{-3}	2.8x10^{-3}
2	30 - 300 eV	5.0x "	3.9x "	3.9x "	3.7x "
3	0.3 - 3 keV	3.9x "	6.0x "	5.7x "	5.2x "
4	3 - 30 keV	2.5x "	9.6x "	9.5x "	9.1x "
5	30 - 300 keV	2.9x "	12.7x "	13.7x "	13.9x "
6	0.3 - 3 MeV	18.2x "	2.9x "	5.4x "	9.1x "

Table 4 - Characteristies of the Geel moderator.

n	Energy	ϵ (sr^{-1})	<d> (cm)	var d (cm^2)	Δ $d_{1/2}$(cm)
1	3 - 30 eV	2.53×10^{-3}	1.7	0.85	2.2
2	30 - 300 eV	3.36x "	1.7	0.87	2.2
3	0.3 - 3 keV	4.85x "	1.9	0.90	2.2
4	3 - 30 keV	7.21x "	2.3	1.08	2.4
5	30 - 300 keV	16.26x "	3.2	1.91	3.3
6	0.3 - 3 MeV	17.63x "	4.6	3.85	4.6

Ω = 49%

Table 5 - Number of degrees of freedom ν of the χ^2-distributions and coefficients of trasformation (6), where the moderation distance d is expressed in cm.

		Normal flight-path				Slanting flight-path			
n	ν	a_0	a_1	a_2	a_3	a_0	a_1	a_2	a_3
1	7.07		0.246				0.244		
2	6.94		0.251				0.249		
3	7.99		0.237				0.234		
4	12.33		0.161	1.0×10^{-3}	5.0×10^{-5}		0.159	1.0×10^{-3}	4.9×10^{-5}
5	17.16		0.154	1.1×10^{-5}	3.0×10^{-5}		0.153	1.1×10^{-3}	3.0×10^{-5}
6	17.43	1.0	0.0797	4.4×10^{-3}	12.9×10^{-5}	1.30	0.0733	4.0×10^{-3}	11.9×10^{-5}

Table 6 - Distribution p(Δl) of the deviation of the effective mean flight-distance for θ = 9°.

3 – 30 eV	p(Δl)		0.14		0.29		0.49		0.71		0.88		0.87		0.47		0.33		0.19		0.09	
	Δl(cm)	-1.0		-0.8		-0.6		-0.4		-0.2		0		0.2		0.5		0.8		1.1		1.4
30 – 300 eV	p(Δl)		0.14		0.52		0.71		0.88		0.87		0.47		0.33		0.19		0.09			
	Δl(cm)	-0.9		-0.7		-0.4		-0.2		0		0.2		0.5		0.8		1.1		1.4		
0.3 – 3 keV	p(Δl)		0.14		0.52		1.05		0.58		0.47		0.33		0.15		0.09					
	Δl(cm)	-0.9		-0.7		-0.4		-0.1		0.2		0.5		0.8		1.2		1.5				
3 – 30 keV	p(Δl)		0.14		0.78		1.59		0.58		0.35		0.25		0.19		0.09					
	Δl(cm)	-0.8		-0.6		-0.4		-0.2		0.1		0.5		0.9		1.2		1.5				
30 – 300 keV	p(Δl)		2.65		0.73		0.24		0.16		0.12		0.06									
	Δl(cm)	-0.4		-0.2		0		0.6		1.2		1.7		2.1								
0.3 – 3 MeV	p (Δl)		0.92		0.45		0.30		0.12		0.06		0.05									
	Δl(cm)	-0.7		-0.2		0.2		0.8		1.6		2.5		3.1								

Table 7 - Distribution p(Δl) of the deviation of the effective mean flight-distance for $\theta = 18^{\circ}$.

Energy												
3 - 30 eV	p(Δl)	0.07	0.14	0.24	0.35	0.44	0.24	0.20	0.12	0.05		
	Δl(cm)	-2.1	-1.7	-1.3	-0.9	0	0.4	1.0	1.5	2.0	2.5	
30 - 300 eV	p(Δl)	0.07	0.14	0.24	0.35	0.58	0.20	0.11	0.05			
	Δl(cm)	-2.1	-1.7	-1.3	-0.9	0	0.3	1.5	2.1	2.6		
0.3 - 3 keV	p(Δl)	0.07	0.19	0.25	0.35	0.44	0.35	0.24	0.19	0.10	0.05	
	Δl(cm)	-2.0	-1.6	-1.3	-0.9	-0.5	-0.1	0.4	1.0	1.5	2.1	2.6
3 - 30 keV	p(Δl)	0.07	0.15	0.32	0.47	0.44	0.29	0.24	0.16	0.10	0.05	
	Δl(cm)	-2.0	-1.6	-1.2	-0.9	-0.6	-0.2	0.4	1.0	1.6	2.2	2.7
30 - 300 keV	p(Δl)	0.09	0.29	0.80	0.59	0.29	0.18	0.12	0.08	0.04		
	Δl(cm)	-1.4	-1.1	-0.9	-0.6	-0.3	0.3	1.1	1.9	2.6	3.3	
0.3 - 3 MeV	p(Δl)	1.58	0.61	0.43	0.13	0.09	0.05	0.04				
	Δl(cm)	-0.8	-0.6	-0.3	0.1	1.2	2.3	3.4	4.2			

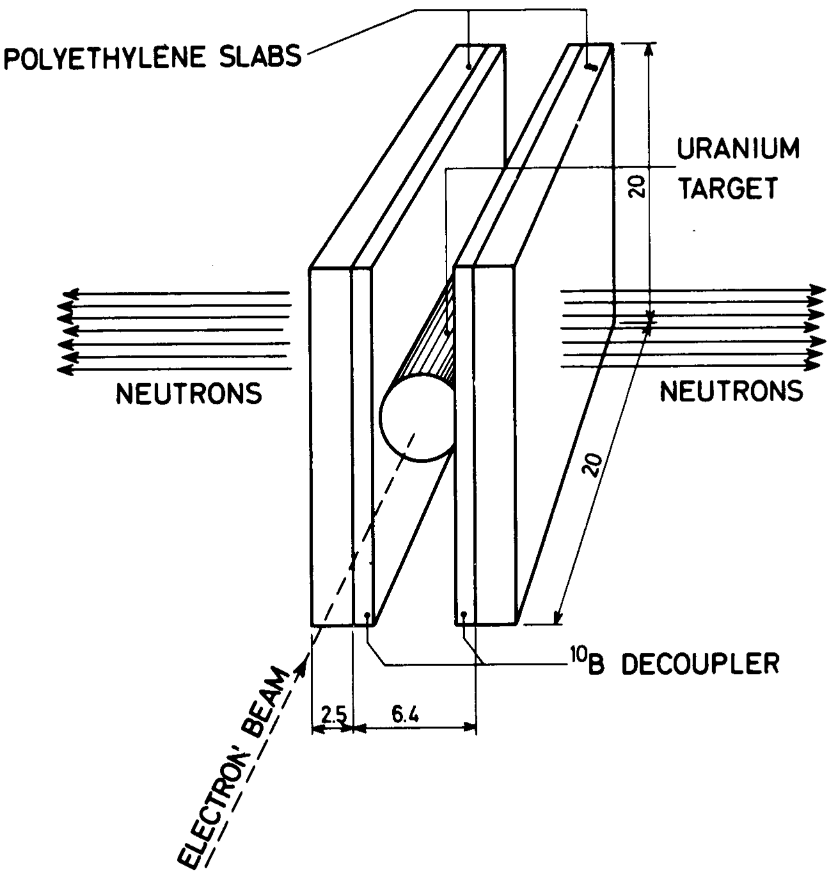

Fig. 1 - Arrangement of the double slab configuration. Dimensions are in cm.

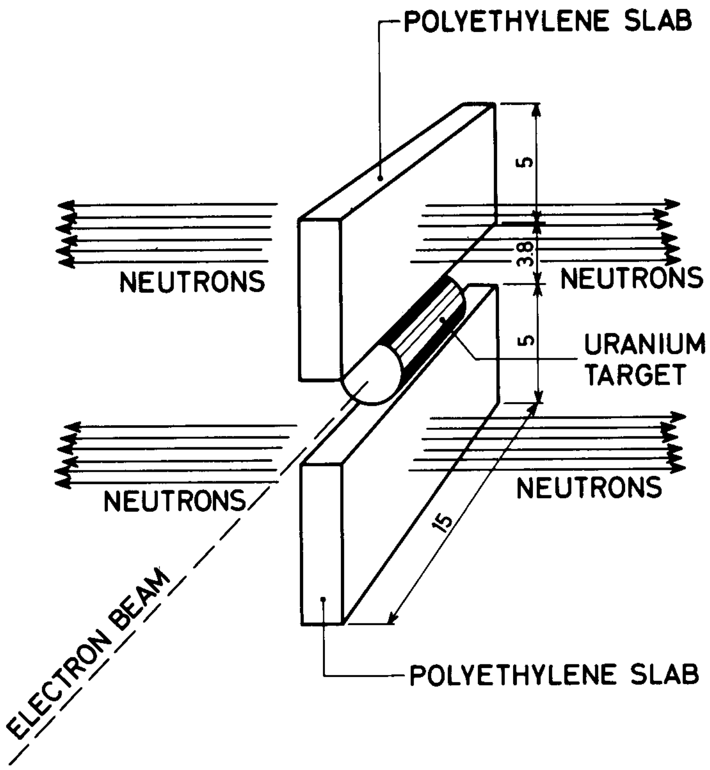

Fig. 2 - Arrangement of the single slab configuration. Dimensions are in cm.

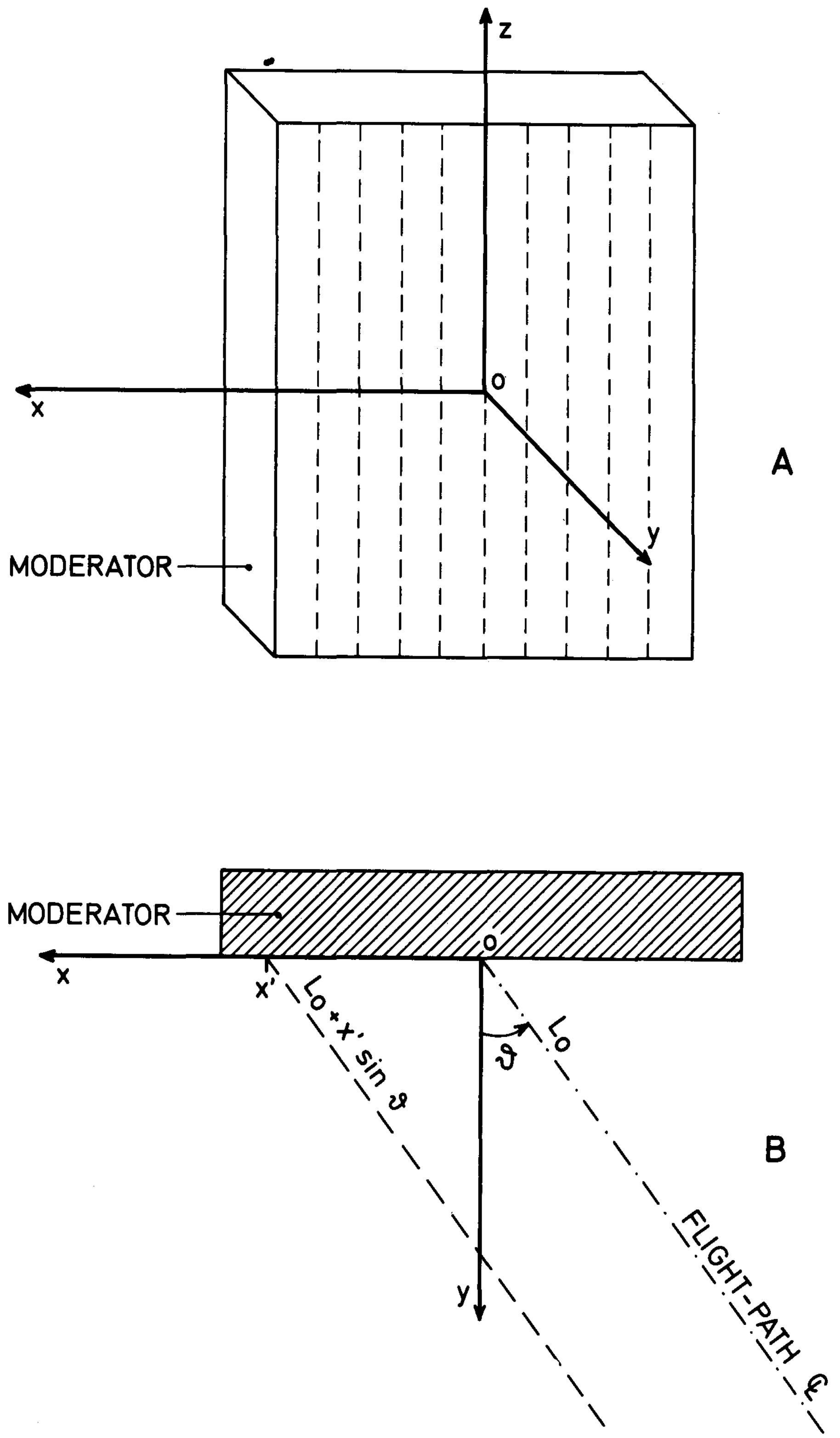

Fig. 3 - Coordinate system. A) The moderator surface facing the flight-paths is divided in ten vertical strips: in each strip ϵ_x, $< d_x >$ and var d_x are calculated separately.
B) The distance of a point at x=x' in the xz plane from the neutron detector is $L_o + x' \sin \theta$, irrespective of z.

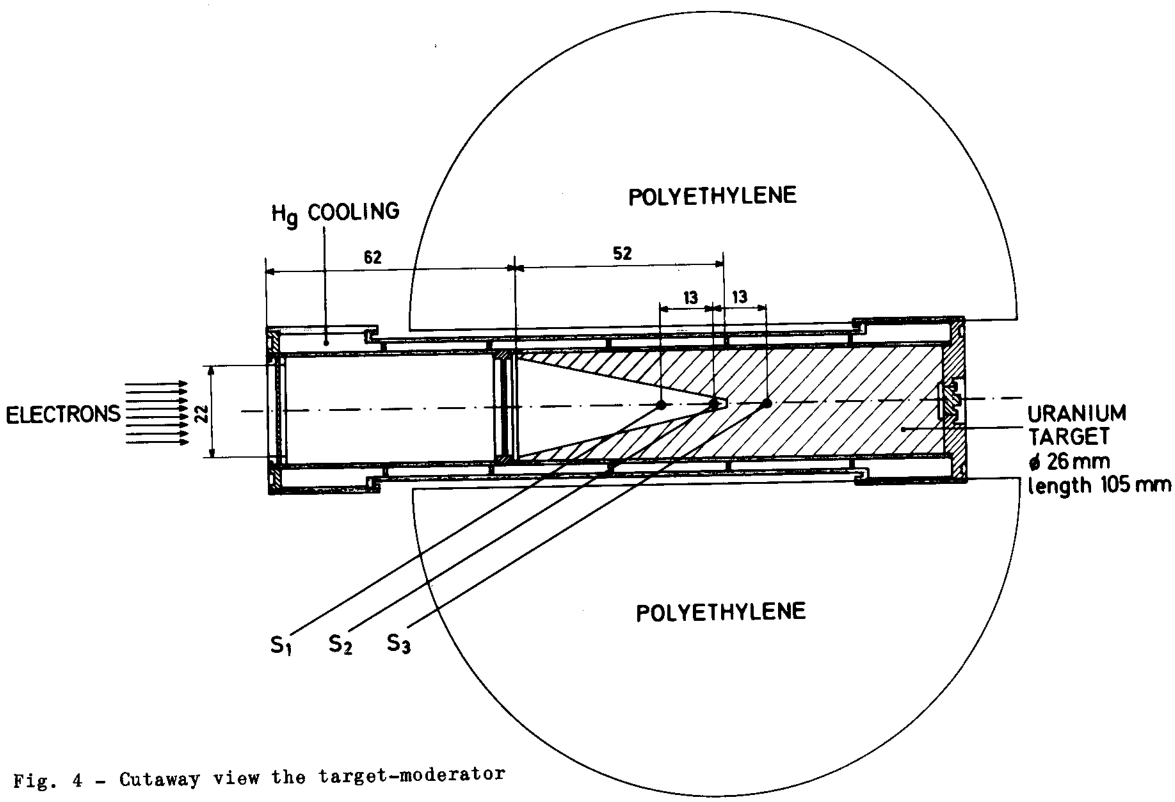

Fig. 4 - Cutaway view the target-moderator assembly of the Geel linac. Approximately 80% of the electron beam current is within a radius of 5 mm from the axis. The extended neutron source is approximated by three point sources S_1, S_2 and S_3. Dimension are in mm.

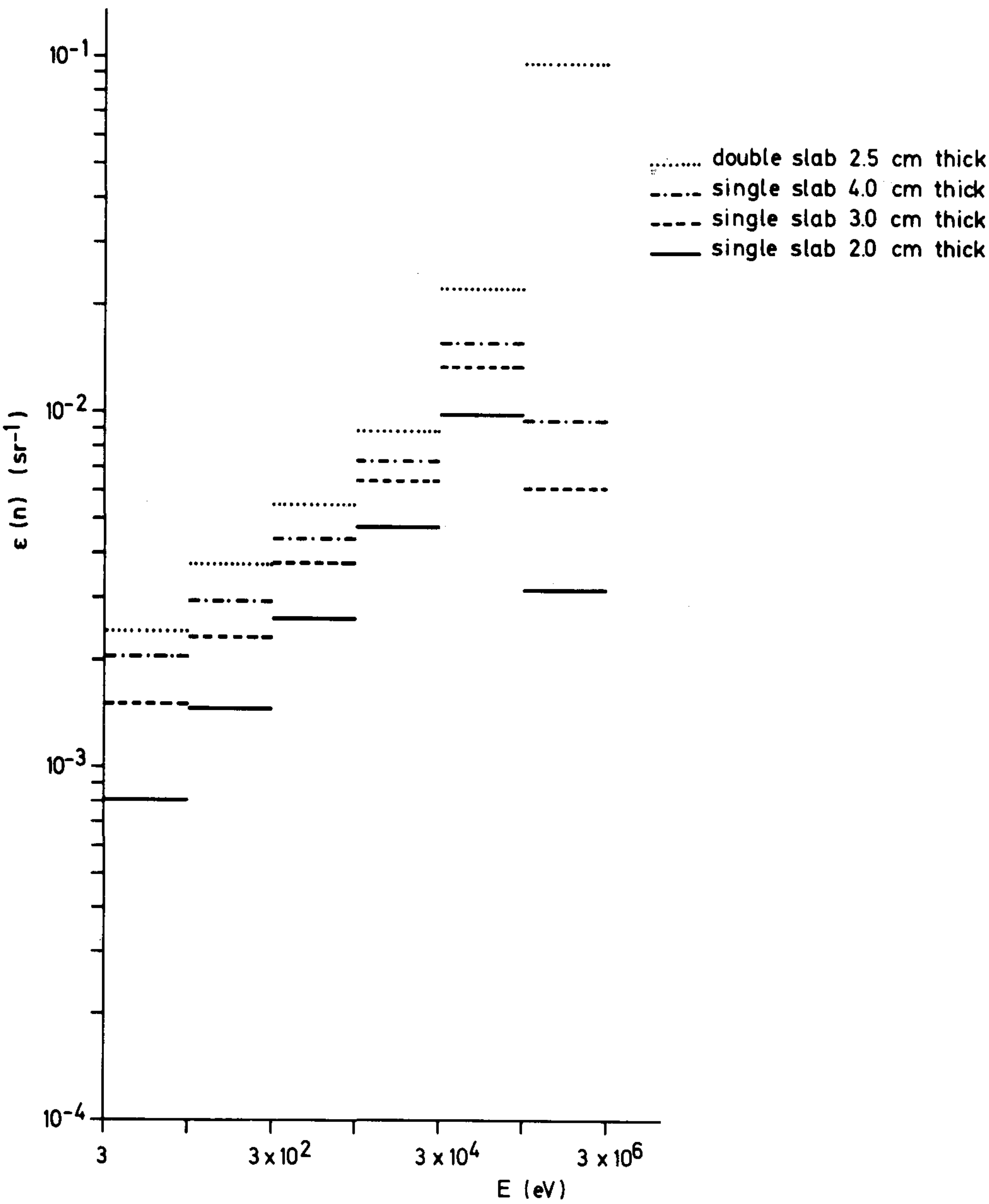

Fig. 5 - Comparison of the moderator efficiencies for double slab and single slab confi - gurations.

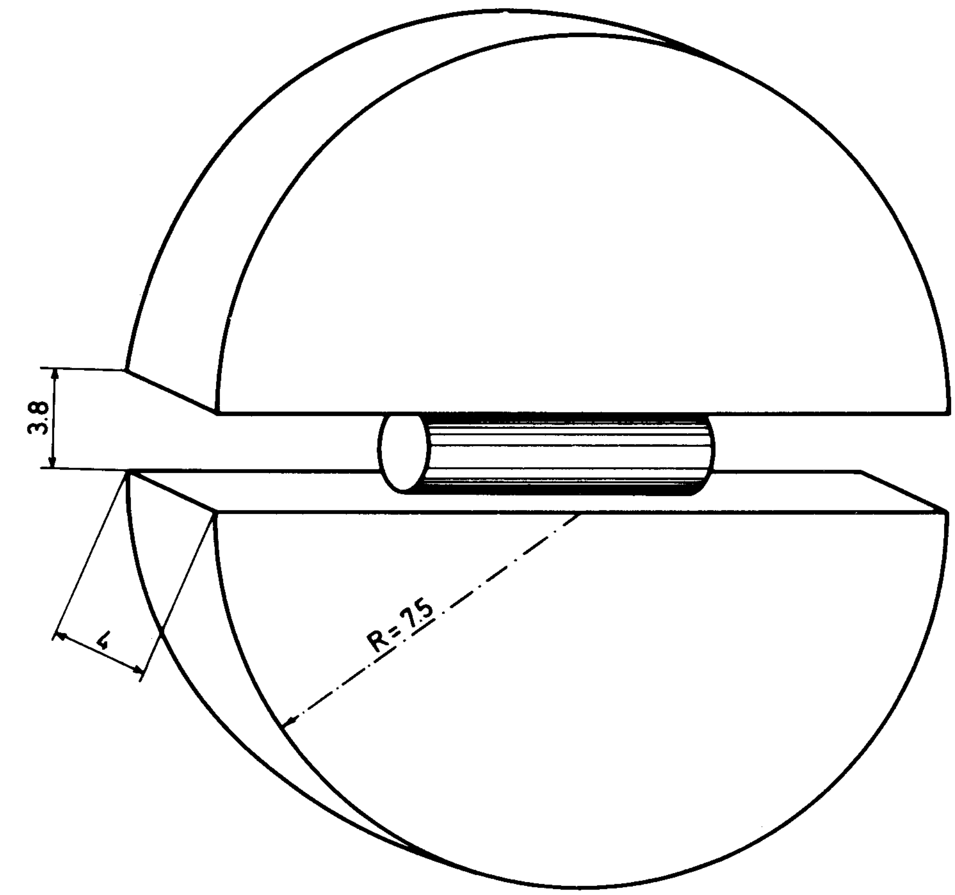

Fig. 6 - Arrangement of the Geel moderator.
Dimensions are in cm.

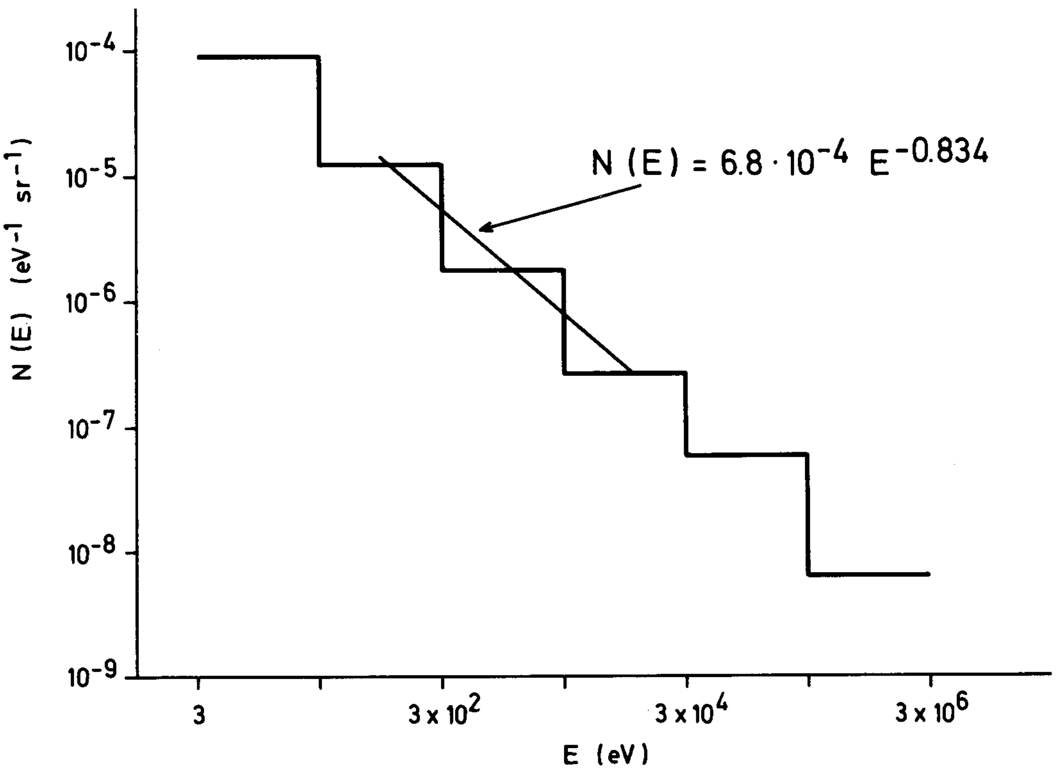

Fig. 7 - Neutron spectrum N(E) calculated for
the disposition of figs. 4 and 6.

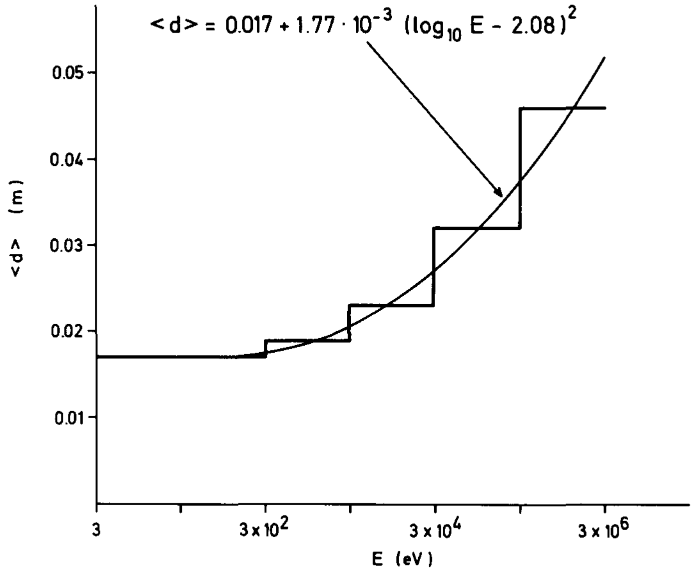

Fig. 8 - Average moderation distance $<d>$ as a function of neutron energy, calculated for the disposition of figs. 4 and 6.

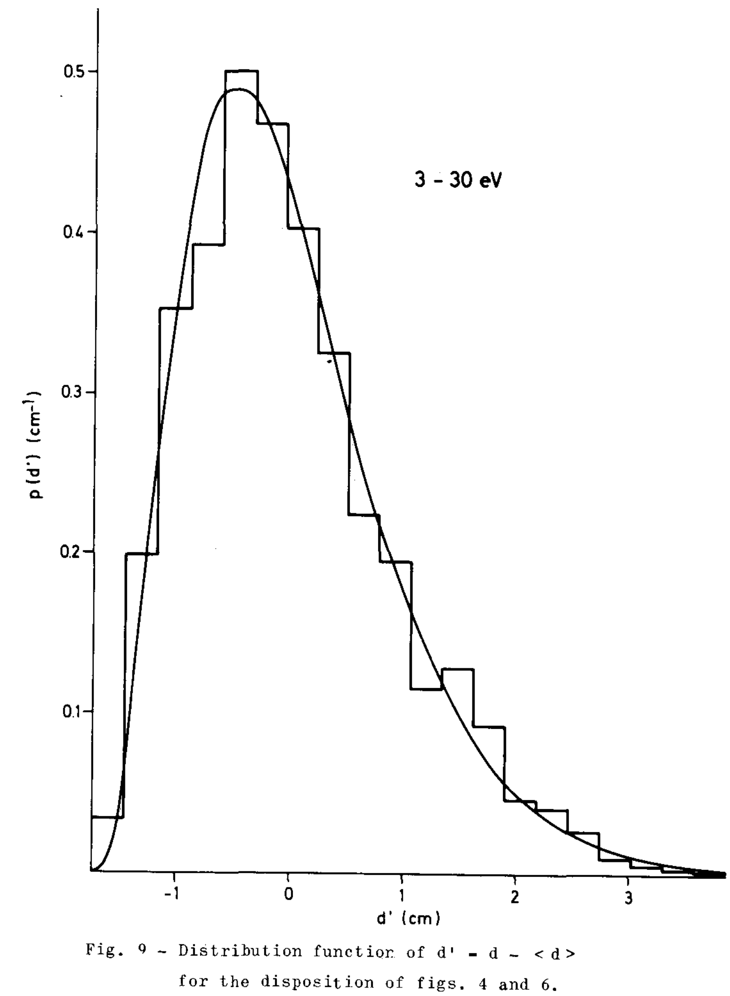

Fig. 9 - Distribution function of $d' = d - <d>$ for the disposition of figs. 4 and 6. The histogram is the output of the Montecarlo calculations; the curve is the fitted χ^2 function. Neutron energy in the interval 3 - 30 eV.

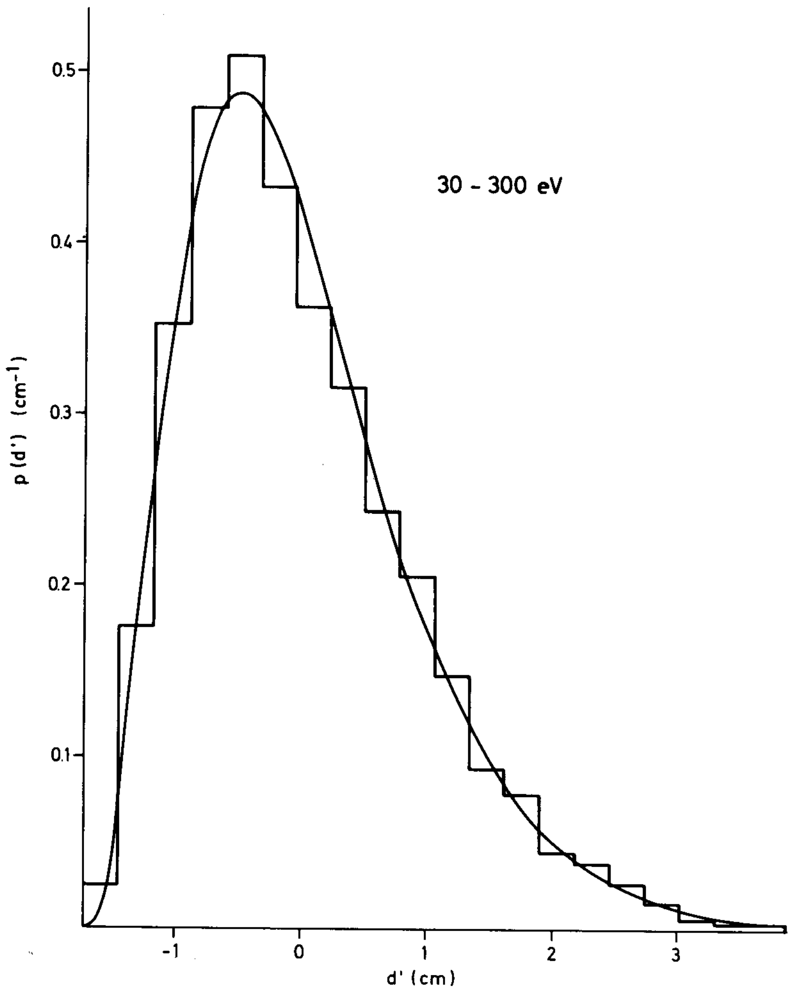

Fig. 10 - Same as fig. 9. Neutron energy in the interval 30 - 300 eV.

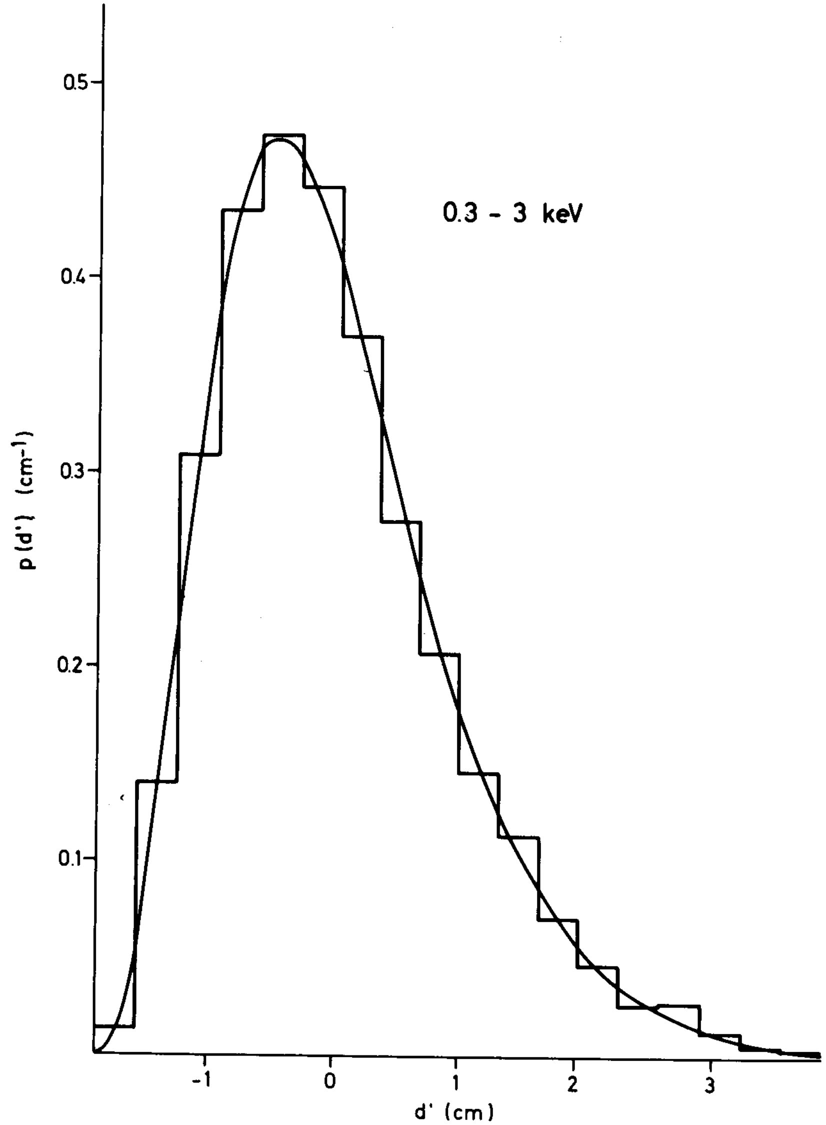

Fig. 11 - Same as fig. 9 Neutron energy in the interval 0.3 - 3 keV.

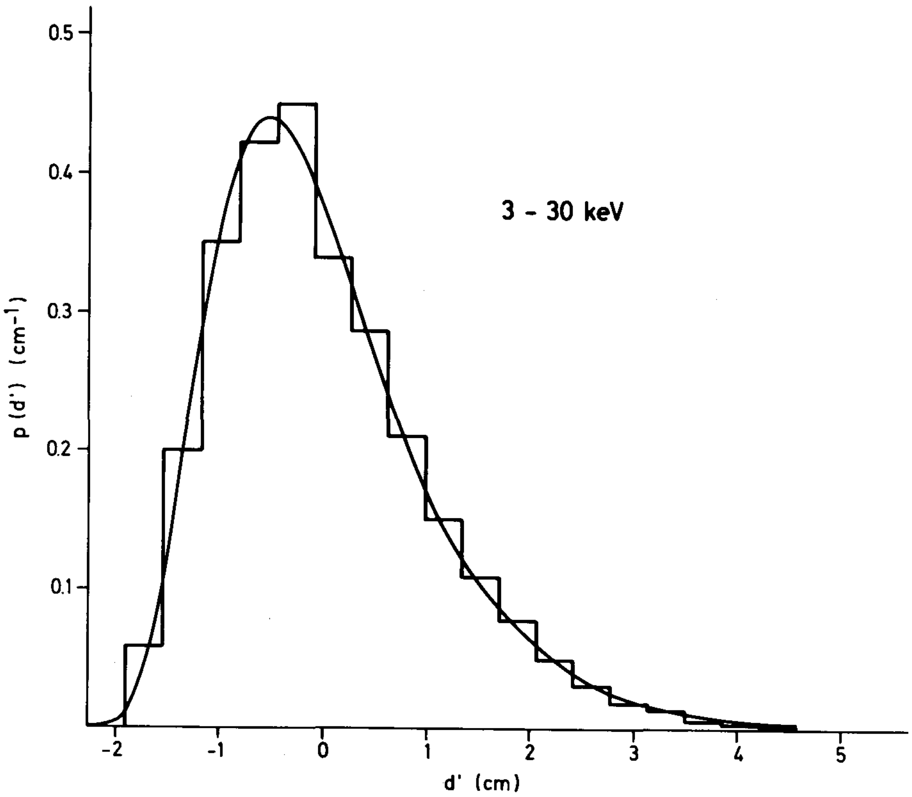

Fig. 12 - Same as fig. 9. Neutron energy in the interval 3 - 30 keV.

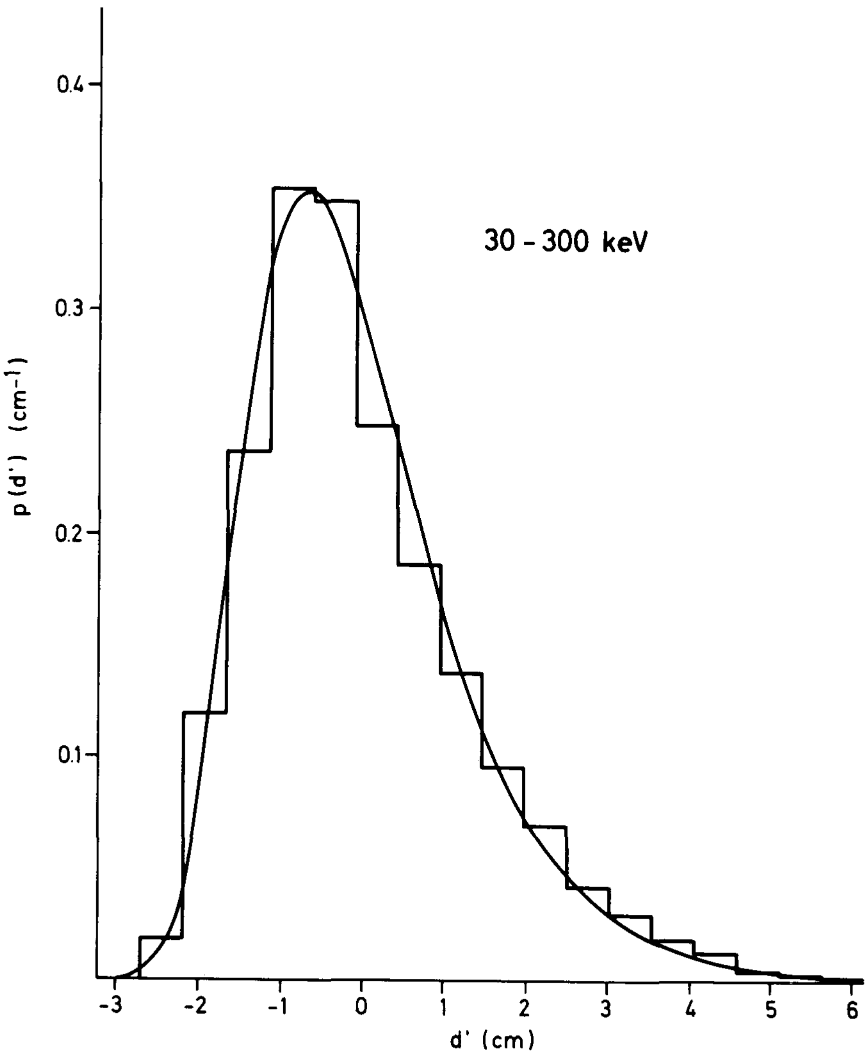

Fig. 13 - Same as fig. 9 Neutron energy in the interval 30 - 300 keV.

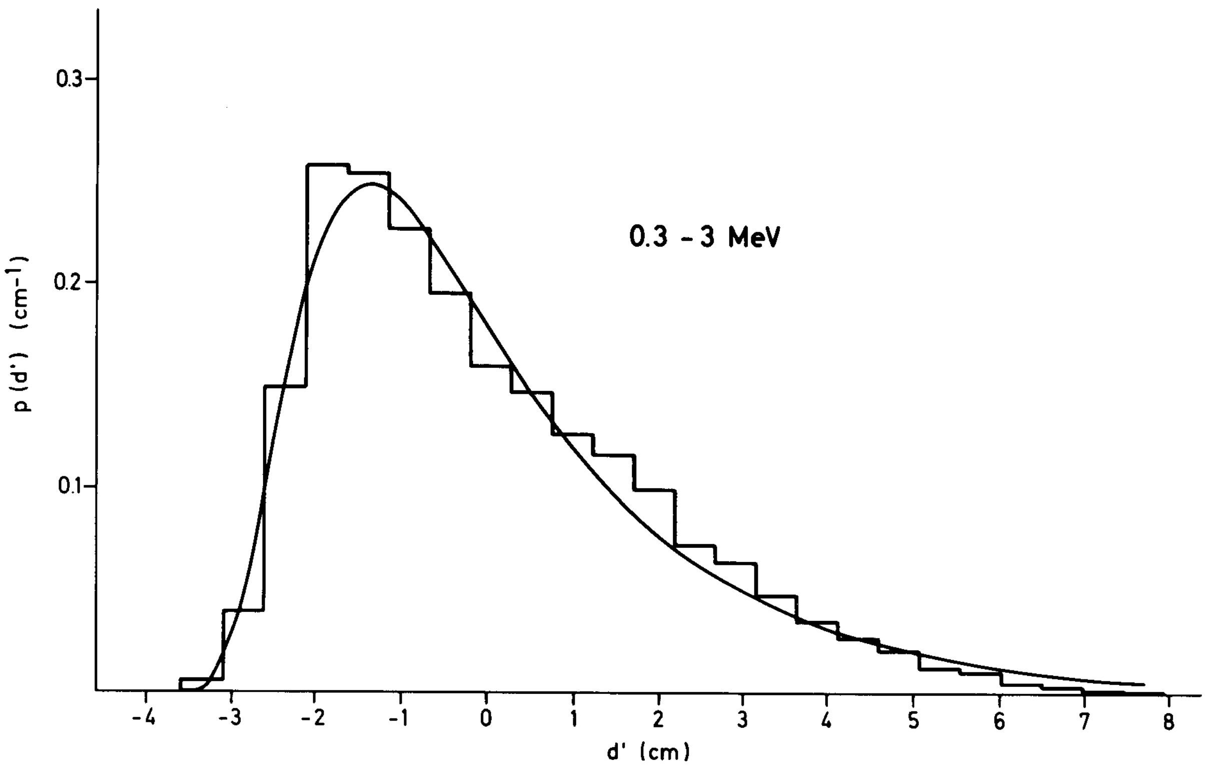

Fig. 14 - Same as fig. 9. Neutron energy in the interval 0.3 - 3 MeV.

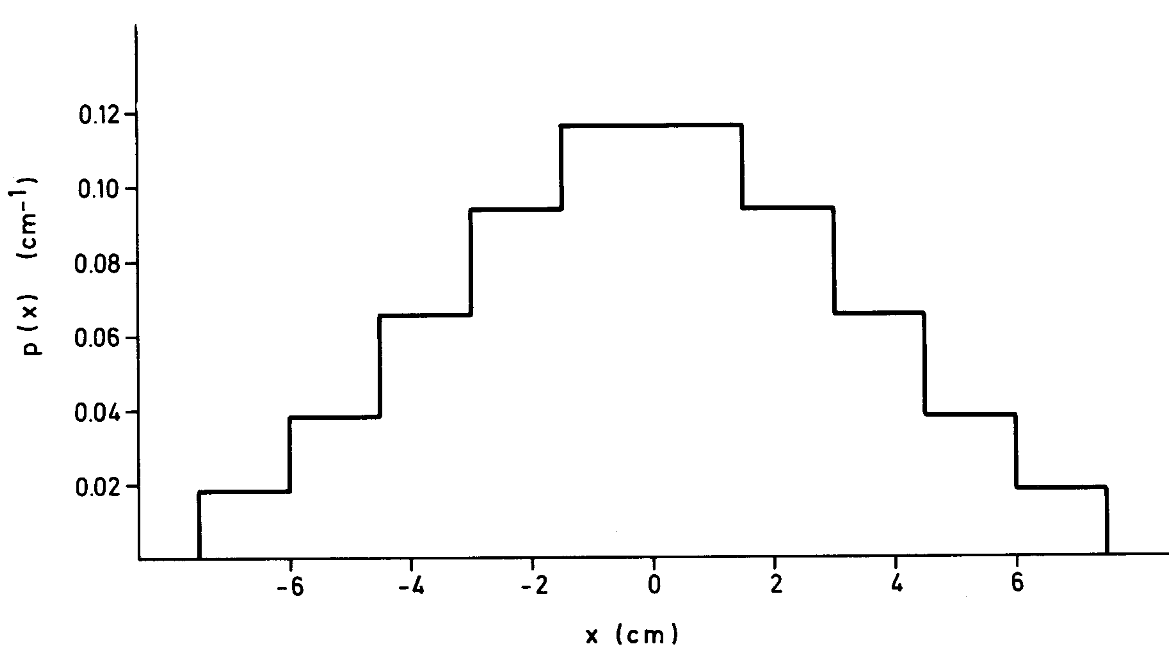

Fig. 15 - Distribution of the escape x-coordinate for the disposition of figs. 4 and 6. This distribution is approximately independent of neutron energy.

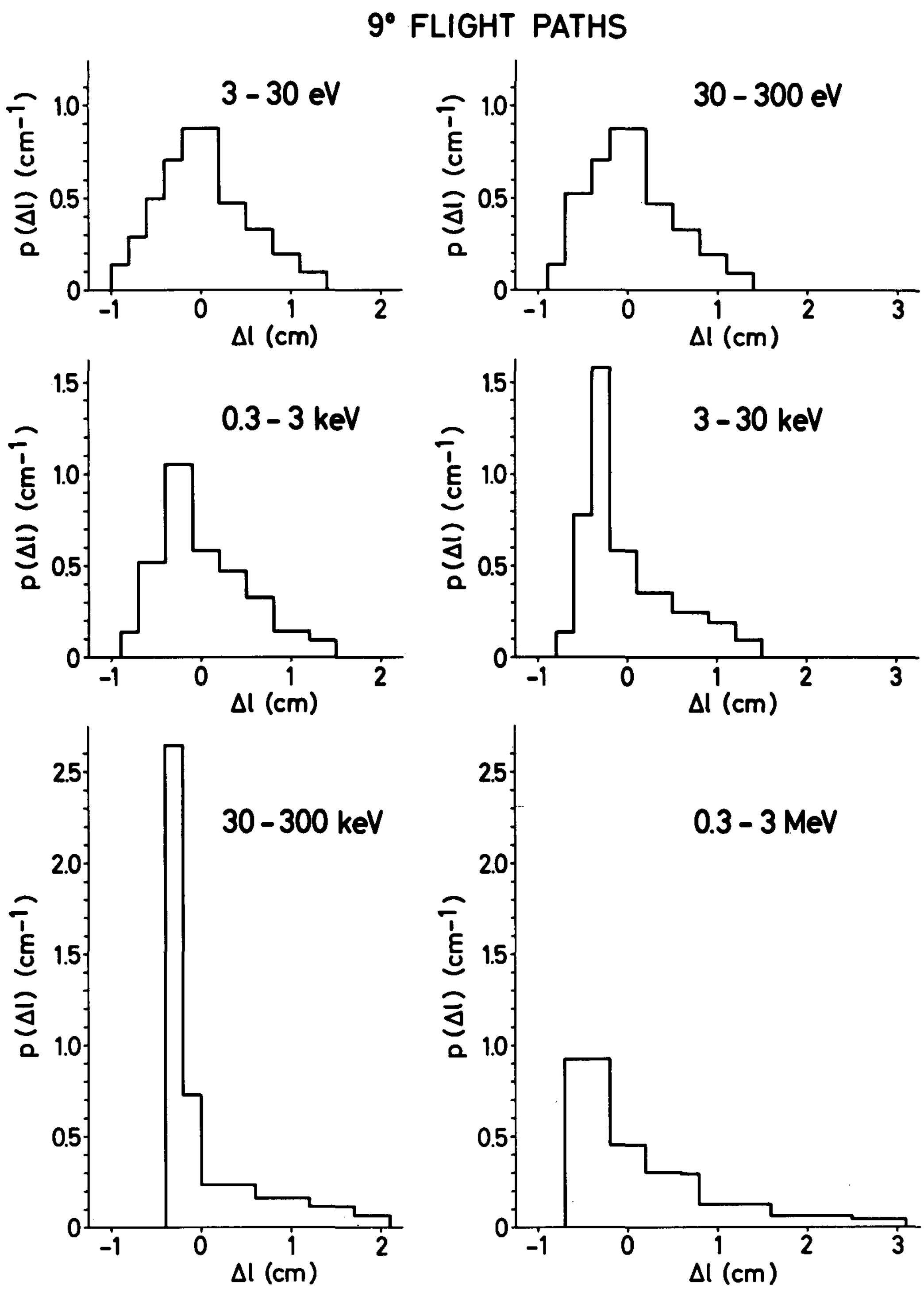

Fig. 16 - Distribution of $\Delta l = \bar{L}_x - \bar{L}$ for slanting flight-paths, for different neutron energies. The moderator disposition is illustrated in figs. 4 and 6. The flight-path angle is $\theta = 9^o$.

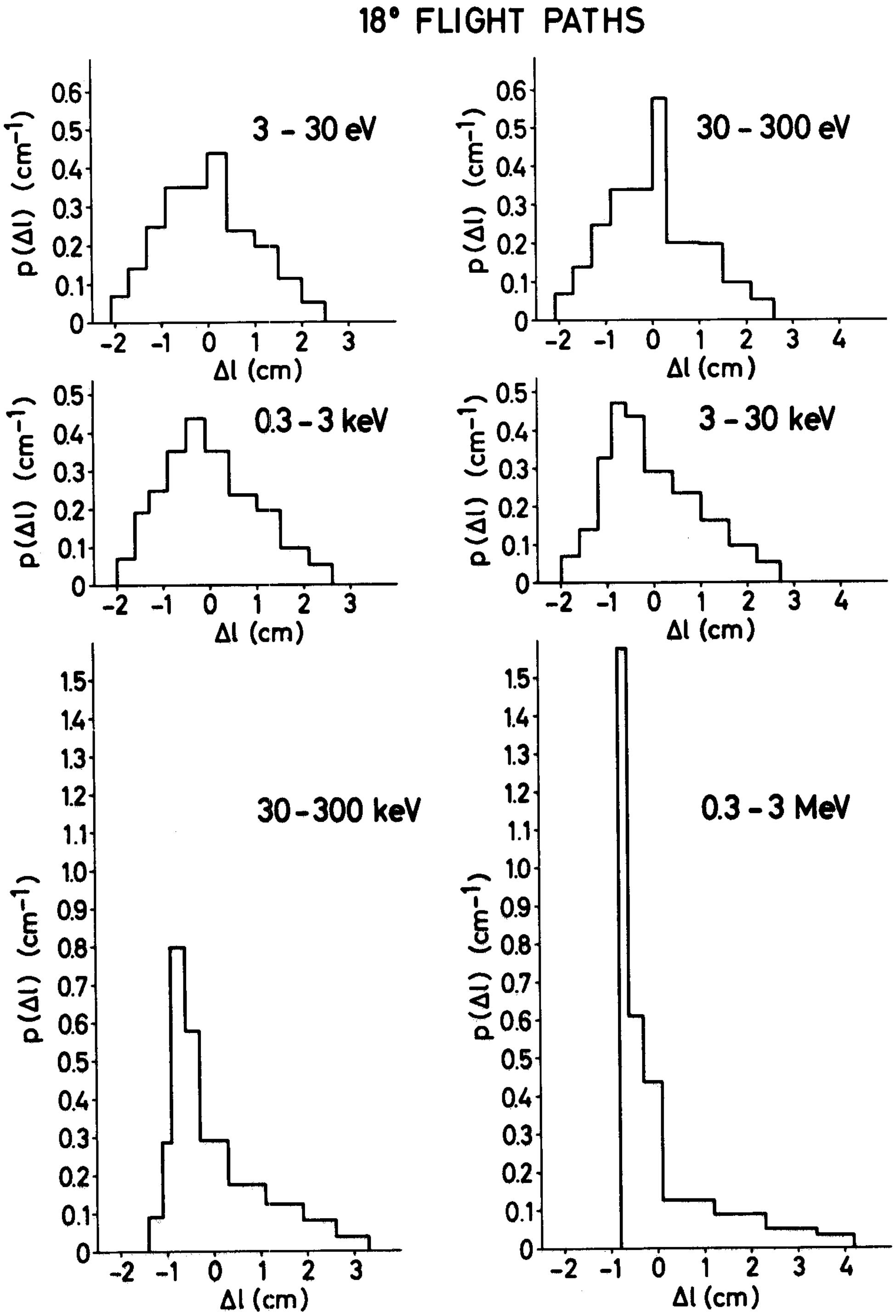

Fig. 17 - Same as fig. 16. Flight-path angle
θ - 18°.

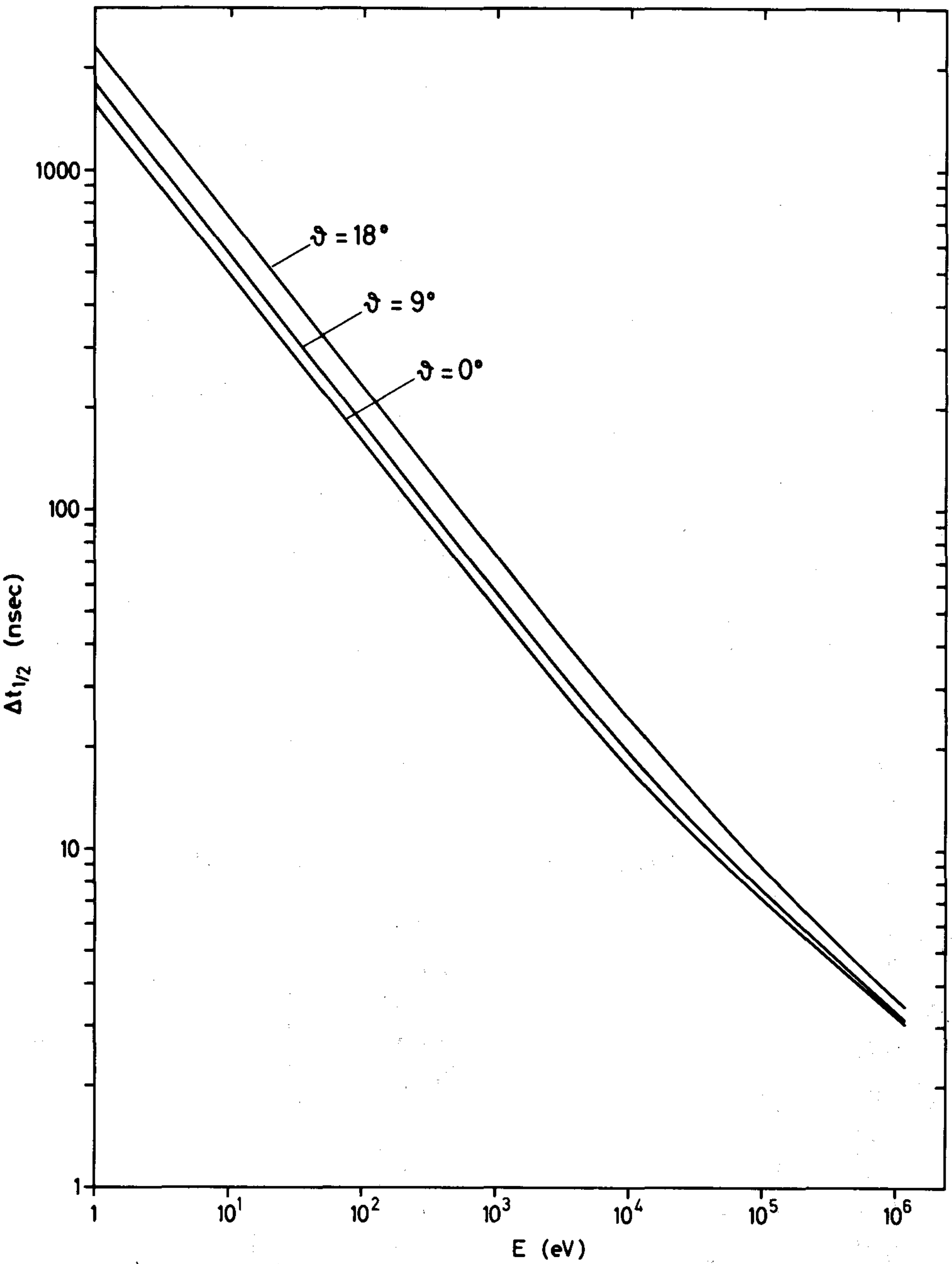

Fig. 18 - Time width of the combined distribution of d and $\bar{L}$ as a function of neutron energy. Indicated is the flight-path angle θ . The curves refer to the set-up illustrated in figs. 4 and 6.

NOTICE TO THE READER

All scientific and technical reports published by the Commission of the European Communities are announced in the monthly periodical **"euro-abstracts"**. For subscription (1 year: B.Fr. 1 025,—) or free specimen copies please write to:

Office for Official Publications
of the European Communities
Boîte postale 1003
Luxembourg 1
(Grand-Duchy of Luxembourg)

To disseminate knowledge is to disseminate prosperity — I mean general prosperity and not individual riches — and with prosperity disappears the greater part of the evil which is our heritage from darker times.

Alfred Nobel

SALES OFFICES

The Office for Official Publications sells all documents published by the Commission of the European Communities at the addresses listed below, at the price given on cover. When ordering, specify clearly the exact reference and the title of the document.

UNITED KINGDOM

H.M. Stationery Office
P.O. Box 569
London S.E. 1 — Tel. 01-928 69 77, ext. 365

BELGIUM

Moniteur belge — Belgisch Staatsblad
Rue de Louvain 40-42 — Leuvenseweg 40-42
1000 Bruxelles — 1000 Brussel — Tel. 12 00 26
CCP 50-80 — Postgiro 50-80

Agency :
Librairie européenne — Europese Boekhandel
Rue de la Loi 244 — Wetstraat 244
1040 Bruxelles — 1040 Brussel

DENMARK

J.H. Schultz — Boghandel
Møntergade 19
DK 1116 København K — Tel. 14 11 95

FRANCE

Service de vente en France des publications des Communautés européennes — Journal officiel
26, rue Desaix — 75 732 Paris - Cédex 15°
Tel. (1) 306 51 00 — CCP Paris 23-96

GERMANY (FR)

Verlag Bundesanzeiger
5 Köln 1 — Postfach 108 006
Tel. (0221) 21 03 48
Telex: Anzeiger Bonn 08 882 595
Postscheckkonto 834 00 Köln

GRAND DUCHY OF LUXEMBOURG

Office for Official Publications of the European Communities
Boite postale 1003 — Luxembourg
Tel. 4 79 41 — CCP 191-90
Compte courant bancaire: BIL 8-109/6003/200

IRELAND

Stationery Office — The Controller
Beggar's Bush
Dublin 4 — Tel. 6 54 01

ITALY

Libreria dello Stato
Piazza G. Verdi 10
00198 Roma — Tel. (6) 85 08
CCP 1/2640

NETHERLANDS

Staatsdrukkerij- en uitgeverijbedrijf
Christoffel Plantijnstraat
's-Gravenhage — Tel. (070) 81 45 11
Postgiro 42 53 00

UNITED STATES OF AMERICA

European Community Information Service
2100 M Street, N.W.
Suite 707
Washington, D.C., 20 037 — Tel. 296 51 31

SWITZERLAND

Librairie Payot
6, rue Grenus
1211 Genève — Tel. 31 89 50
CCP 12-236 Genève

SWEDEN

Librairie C.E. Fritze
2, Fredsgatan
Stockholm 16
Post Giro 193, Bank Giro 73/4015

SPAIN

Libreria Mundi-Prensa
Castello 37
Madrid 1 — Tel. 275 51 31

OTHER COUNTRIES

Office for Official Publications of the European Communities
Boite postale 1003 — Luxembourg
Tel. 4 79 41 — CCP 191-90
Compte courant bancaire: BIL 8-109/6003/200

OFFICE FOR OFFICIAL PUBLICATIONS OF THE EUROPEAN COMMUNITIES
Boite postale 1003 — Luxembourg
6546